Exposure to cAMP and β-adrenergic stimulation recruits Ca_V3 T-type channels in rat chromaffin cells through Epac cAMP-receptor proteins

M. Novara, P. Baldelli, D. Cavallari, V. Carabelli, A. Giancippoli and E. Carbone

Department of Neuroscience, INFM Research Unit, 10125 Torino, Italy

T-type channels are expressed weakly or not at all in adult rat chromaffin cells (RCCs) and there is contrasting evidence as to whether they play a functional role in catecholamine secretion. Here we show that 3–5 days after application of pCPT-cAMP, most RCCs grown in serum-free medium expressed a high density of low-voltage-activated T-type channels without altering the expression and characteristics of high-voltage-activated channels. The density of cAMP-recruited T-type channels increased with time and displayed the typical biophysical and pharmacological properties of low-voltage-activated Ca^{2+} channels: (1) steep voltage-dependent activation from −50 mV in 10 mM Ca^{2+}, (2) slow deactivation but fast and complete inactivation, (3) full inactivation following short conditioning prepulses to −30 mV, (4) effective block of Ca^{2+} influx with 50 μM Ni^{2+}, (5) comparable permeability to Ca^{2+} and Ba^{2+}, and (6) insensitivity to common Ca^{2+} channel antagonists. The action of exogenous pCPT-cAMP (200 μM) was prevented by the protein synthesis inhibitor anisomycin and mimicked in most cells by exposure to forskolin and 1-methyl-3-isobutylxanthine (IBMX) or isoprenaline. The protein kinase A (PKA) inhibitor H89 (0.3 μM) and the competitive antagonist of cAMP binding to PKA, Rp-cAMPS, had weak or no effect on the action of pCPT-cAMP. In line with this, the selective Epac agonist 8CPT-2Me-cAMP nicely mimicked the action of pCPT-cAMP and isoprenaline, suggesting the existence of a dominant Epac-dependent recruitment of T-type channels in RCCs that may originate from the activation of β-adrenoceptors. Stimulation of β-adrenoceptors occurs autocrinally in RCCs and thus, the neosynthesis of low-voltage-activated channels may represent a new form of 'chromaffin cell plasticity', which contributes, by lowering the threshold of action potential firing, to increasing cell excitability and secretory activity during sustained sympathetic stimulation and/or increased catecholamine circulation.

(Received 15 January 2004; accepted after revision 6 May 2004; first published online 14 May 2004)
Corresponding author E. Carbone: Department of Neuroscience, INFM Research Unit, 10125 Torino, Italy. Email: emilio.carbone@unito.it

Expression and modulation of voltage-gated Ca^{2+} channels are critical determinants for controlling Ca^{2+} entry and Ca^{2+}-dependent exocytosis in adrenal chromaffin cells. Two decades of work have shown that Ca^{2+} channels belonging to Ca_V1 and Ca_V2 channel families (L-, N-, P/Q-, R-types) largely control the voltage-dependent Ca^{2+} influx in bovine and rat chromaffin cells (BCCs, RCCs) and the corresponding catecholamine release (García *et al.* 1984; Albillos *et al.* 1994, 2000; Artalejo *et al.* 1994; Engisch & Nowycky, 1996; Carabelli *et al.* 2003). Only in 50% of developing immature RCCs (Bournaud *et al.* 2001) and in a small fraction of adult RCCs (Hollins & Ikeda, 1996), Ca_V3 channels (T-type) are shown to contribute to a transient inward Ca^{2+} current. This is intriguing since: (1) T-channels are expressed in the most excitable cells of young and adult animals (Perez-Reyes, 2003), (2) T-channels support the generation of action potential in adrenal glomerulosa and zona fasciculata cells (Barbara & Takeda, 1995; Schrier *et al.* 2001), and (3) the mRNA of $Ca_V3.1$ and $Ca_V3.2$ channels (α_{1G}, α_{1H}) is readily available in BCCs (García-Palomero *et al.* 2000). Thus, expression of functional T-type channels may be critically linked to the regulation of some extracellular or cytoplasmic factor, capable of triggering gene transcription, protein synthesis and channel membrane incorporation.

 DOI: 10.1113/jphysiol.2004.061184

Various reports indicate that cAMP-dependent pathways are critical elements for recruiting $GABA_A$ receptors (Thompson *et al.* 2000) and voltage-gated Na^+ and Ca^{2+} channels (Yuhi *et al.* 1996; Beaudu-Lange *et al.* 1998; Doležal *et al.* 2001; Mariot *et al.* 2002) in neurones, glial and neuroendocrine cells. In the case of chromaffin cells, several reports suggest that the basal levels of cAMP are low but can rise following adenylate cyclase activation, phosphodiesterase inhibition or β-adrenoceptor (β-AR) stimulation (Parramón *et al.* 1995; Carabelli *et al.* 2001; Carbone *et al.* 2001). On the other hand, RCCs express heterogeneous densities of β_1- and β_2-ARs exerting distinct action on Ca^{2+} channels: β_1-ARs up-regulate the activity of L-channels via a cAMP/PKA pathway while β_2-ARs produce fast inhibition of L- and non-L-currents via PTX-sensitive $G_{i,o}$-proteins (Cesetti *et al.* 2003). The existence of an autocrine modulatory pathway capable of elevating cAMP during exposures to β-AR agonists raises the questions of: (a) whether sustained elevations of cAMP or β-AR stimulation could induce the recruitment of newly available Ca^{2+} channels, and (b) what may be the role of PKA-dependent and PKA-independent pathways in this process. These issues are of relevance for understanding the long-term autocrine control of catecholamine release during sustained sympathetic stimulation of adrenal glands ('fight or flight' response).

Here we show that exposure to pCPT-cAMP or β-AR stimulation are both capable of producing a selective recruitment of newly available Ca_V3 channels with no changes of the dominant Ca_V1 and Ca_V2 families. The cAMP-mediated recruitment of T-type channels requires 3–5 days to reach maximal levels and is mainly mediated by a PKA-independent signalling pathway through the cAMP-receptor protein Epac ((cAMP-guanine nucleotide exchange factor) cAMP-GEF). Availability of newly recruited T-type channels drastically lowers the threshold of chromaffin cell excitability during action potential firing. This, together with the increased exocytosis occurring at low voltages (Giancippoli *et al.* 2004), suggests that the cAMP-dependent recruitment of low-voltage-activated Ca^{2+} channels represents an effective mechanism through which chromaffin cells self-potentiate their activity during sustained sympathetic stimulation.

Methods

Isolation and culture of RCCs

Chromaffin cells were obtained from the adrenal glands of adult Sprague-Dawley rats (200–300 g) killed by cervical dislocation. All experiments were carried out in accordance with the guidelines established by the National Council on Animal Care and were approved by the local Animal Care Committee of Turin University. Cell preparation was achieved as previously described (Hernández-Guijo *et al.* 1999). To avoid contamination of cortical tissues, the isolation of chromaffin cells was limited to a narrow region of the adrenal medullae, which drastically reduced the number of available cells. Cells were plated on plastic dishes pretreated with poly-L-ornithine (1 mg ml^{-1}) and laminin (5 μg ml^{-1} in L-15 carbonate), incubated at 37°C in a water-saturated atmosphere with 5% CO_2 and used within 2–6 days of plating. The culture medium was made serum-free to prevent different batches from inducing different effects on the recruitment of T-type channels (see Beaudu-Lange *et al.* 1998). The medium contained: Dulbecco's modified Eagle's medium (DMEM), penicillin–streptomycin 0.5% and gentamycin 0.25%, and was not changed during the culture period. Cultured cells were allowed to adhere for 24 h from plating, after which the membrane-permeable cAMP analogue pCPT-cAMP (200 μM), isoprenaline (1 μM) + ascorbic acid (100 μM) or forskolin (10 μM) + IBMX (10 μM) were added. Cells were maintained for up to 6 days in the culture medium and were no longer exposed to the above compounds.

Electrophysiological recordings

Ca^{2+} currents and action potential recordings were performed with an Axopatch 200A (Axon Instruments, Union City, CA, USA) and an EPC-9 patch-clamp amplifier (HEKA-Electronic, Lambrecht, Germany) using the corresponding software (pCLAMP and PULSE). Pipettes were obtained from thin Kimax borosilicate glass (Witz Scientific, Holland, OH, USA) and fire-polished to obtain a final series resistance of 2–3 MΩ for currents and action potential recordings.

Voltage-clamp recordings. Ca^{2+} currents were measured in the whole-cell configuration as previously described (Hernández-Guijo *et al.* 1999). The currents were evoked either by step depolarizations of 20–100 ms to a variable potential from −50 to +40 mV or by ramp commands from −60 to +80 mV with a slope of 0.9 V s^{-1} (sampled at 5–10 kHz and low-pass filtered at 2 kHz). During tail current recordings the signals were sampled at 20–40 kHz and filtered at 5 kHz. The holding potential (V_h) was usually set at −80 mV. Fast capacitative transients during step depolarizations were minimized online by the patch-clamp analog compensation. Uncompensated capacitative currents were further reduced by subtracting the averaged currents

in response to $P/4$ hyperpolarizing pulses. Cells with leak current greater than 15 pA at holding potential were excluded from the analysis. Series resistance was compensated by 80% and monitored throughout the experiment. Since the drugs applied to the external solution did not significantly affect the liquid junction potential (LJP), the indicated voltages were not corrected for the LJP at the interface between the pipette solution and the bath.

Current-clamp recordings. Action potentials were recorded in current-clamp mode using the perforated-patch configuration and solutions of approximately physiological ionic composition (see below). Series resistances between 15 and 10 MΩ were reached 10–15 min after seal formation. Resting membrane potentials ranged between −55 and −60 mV. To stop the spontaneous firing that was sometimes present with no current injection, cells were maintained at a holding potential between −70 and −90 mV by injecting variable amounts of steady holding currents (−3 to −20 pA). At these voltages, the cell input resistance measured with hyperpolarizing current pulses was high in both cAMP-untreated and cAMP-treated RCCs (0.3–0.7 GΩ). To elicit action potential firing, cells were depolarized by injecting current steps of different duration and amplitude. Action potentials were acquired at 5 kHz and low-pass filtered at 2.5 kHz. Action potential detection and complete waveform analysis was performed with Minianalysis Software (Synaptosoft, Leonia, NJ, USA). The threshold was set by the program as the location of the 3rd differential peak during the rising phase of the action potential.

Experiments were performed at room temperature (22–24°C). Data are given as mean ± S.E.M. for n = number of cells. Statistical significance was calculated using unpaired Student's t test and P values < 0.05 were considered significant.

Solutions

Ca^{2+} currents were recorded in the whole-cell configuration by superfusing the cells with an external solution containing (mM): 10 $CaCl_2$, 137 Tris-HCl, 4 KCl, 1 $MgCl_2$, 10 Hepes (pH 7.4 with KOH). The standard internal solution was (mM): 100 CsCl, 20 TEACl, 10 EGTA, 2 $MgCl_2$, 8 glucose, 4 ATP, 0.5 GTP, 15 phosphocreatine, 10 Hepes (pH 7.4 with CsOH). Action potentials were recorded in the perforated-patch configuration with external solutions containing (mM): 140 NaCl, 4 KCl, 2 $CaCl_2$, 1 $MgCl_2$, 10 Hepes (pH 7.4 with NaOH). The pipette solution contained (mM): 135 potassium aspartate, 8 NaCl, 2 $MgCl_2$, 20 Hepes (pH 7.3 with KOH) and 50–100 μg ml^{-1} amphotericin B. The handling of amphotericin B (Sigma, St Louis, MO, USA) and the procedure to optimize the perforated-patch conditions were described elsewhere (Cesetti *et al.* 2003; Carabelli *et al.* 2003). pCPT-cAMP, Rp-adenosine 3′,5′-cyclic-monophosphorothioate triethylammonium salt (Rp-cAMPS), 8-(4-chlorophenylthio)-2′-*O*-methyl-adenosine 3′,5′-cyclic monophosphate sodium salt (8CPT-2Me-cAMP), nifedipine, isoprenaline, forskolin, 1-methyl-3-isobutylxanthine (IBMX), KN-93 and anisomycin were purchased from Sigma. The PKA inhibitor H89 was obtained from CN Biosciences Inc. (Darmstadt, Germany). ω-CTx-GVIA, ω-Aga-IVA toxins and SNX-482 were purchased from the Peptide Institute (Osaka, Japan) and prepared to the final concentration as previously described (Magnelli *et al.* 1998).

Results

Figure 1*A* shows a series of Ca^{2+} currents recorded from a cAMP-untreated RCC in the whole-cell configuration and bathed in 10 mM Ca^{2+}. Nifedipine (1 μM) was added to block the L-type channels, which carry half of the high-voltage-activated (HVA) Ca^{2+} current in RCCs (Gandía *et al.* 1995). The solution also contained TTX (300 nM) and $Tris^+$ as substitutes for Na^+ to block all types of Na^+ currents (TTX-sensitive and TTX-resistant). Under these conditions, depolarizations from −50 to +40 mV in 10 mV steps revealed the presence of only slowly inactivating Ca^{2+} currents, which started activating at around −20 mV with fast activation kinetics and maximal amplitudes between +10 and +20 mV. As previously reported (Cesetti *et al.* 2003), in most of the cells tested (91%, $n = 134$) there was no sign of low-voltage-activated (LVA) Ca^{2+} currents, which were expected to activate at around −40 mV under the present ionic conditions. The current–voltage (I–V) characteristics of nifedipine-resistant Ca^{2+} currents, either determined from sequential step depolarizations or ramp commands, had only a single negative peak at about +18 mV and showed no sign of a second 'shoulder' peaking at about −20 mV, which would have been strong evidence for the presence of LVA T-type currents (Carbone & Lux, 1984*a*).

cAMP uncovers a transient LVA T-type current

Three to five days after the addition of the membrane-permeable cAMP analogue pCPT-cAMP (200 μM) to the culture medium, the RCCs displayed a sizeable T-type current, which was evident in isolation between −40 and

−20 mV and contributed to most of the fast current decay at more positive potentials (Fig. 1*B*). In line with this, the *I–V* curves obtained by ramp commands showed the typical 'shoulder' of the T-type current peaking at around −20 mV (arrows in Fig. 1*C* and *D*). Notice that, due to the transient nature of T-type channels, a ramp command does not permit a faithful representation of the *I–V* characteristics but allows a clearer separation of the fast inactivating T-type current from the slowly inactivating HVA component.

To assess the real identity of the T-type current we first compared the blocking action of Ni^{2+} and Cd^{2+} and examined the effects of replacing Ca^{2+} with Ba^{2+} (Carbone & Lux, 1987; Fox *et al.* 1987). Figure 1*C* shows that 50 μM Ni^{2+} selectively blocked the cAMP-recruited T-type current measured during ramp commands or step-depolarizations, while 30 μM Cd^{2+} preferentially blocked the slowly inactivating nifedipine-insensitive HVA currents (Fig. 1*D*). On average, 50 μM Ni^{2+} blocked $72 \pm 3\%$ ($n = 8$) of the fast inactivating component at −30 mV and the overall blocking potency of Ni^{2+} was well fitted with a single dose-dependent relationship with $IC_{50} = 16\ \mu$M (Fig. 2*A*). Figure 2*B* shows that the time course and amplitude of the fast inactivating current recruited by long-term exposure to cAMP (indicated as I_t and calculated after subtraction of the steady-state

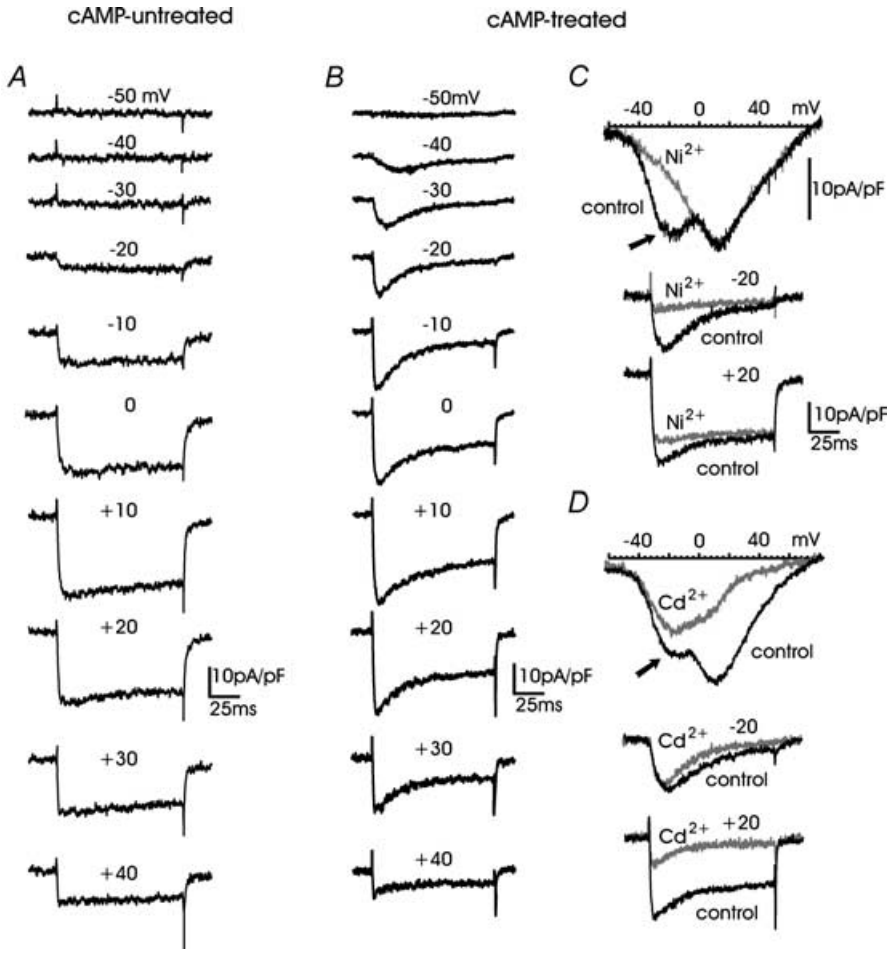

Figure 1. Time course of Ca^{2+} currents in cAMP-treated and cAMP-untreated RCCs: distinct blocking action of Ni^{2+} and Cd^{2+}

A, Ca^{2+} currents recorded during consecutive step depolarizations at the indicated voltages from a 4 day RCC cultured in the absence of pCPT-cAMP. Holding potential (V_h) and return potential (V_r) were −80 mV. *B*, same recording conditions as in *A* from a 5 day RCC exposed since the 1st day of culture to 200 μM pCPT-cAMP. *C*, 50 μM Ni^{2+} blocked the 'low-threshold shoulder' of the *I–V* curve (arrow) and the currents recorded at −20 and +20 mV (grey traces). Ni^{2+}-insensitive currents were no longer fast inactivating. *D*, addition of 30 μM Cd^{2+} blocked the high-threshold component of the *I–V* curve and the stationary currents recorded during step depolarizations. Cd^{2+}-insensitive currents were fast, fully inactivating and preserved the 'low-threshold shoulder' of the *I–V* curve (arrow). Same conditions and scale bars as in *C*.

component, I_{ss}) remained unchanged when replacing Ca^{2+} with Ba^{2+}. In contrast, there was a net increase of I_{ss} between −20 mV and +20 mV ($P < 0.016$), which derived from the higher permeability of HVA channels to Ba^{2+} with respect to Ca^{2+} (Almers & McCleskey, 1984). Taken all together, these data support the idea that pCPT-cAMP effectively recruits a significant T-type current.

Long-term exposure to cAMP recruits LVA but not HVA channel types

Given that cAMP recruits T-type channels, in a series of preliminary experiments we studied the optimal conditions of long-term recruitment. We found that the optimal concentration of pCPT-cAMP was 200 μM. With lower concentrations (50–100 μM), the percentage of cells with T-type currents was drastically reduced and current densities were significantly smaller (not shown). Higher concentrations (500 μM to 1 mM) had comparable effects to 200 μM. We then examined how the morphology, the cell size (membrane capacitance, pF) and the amplitude of T-currents at −30 mV changed with the day of culture, focusing on healthy responsive RCCs with no bias toward a specific cell size. Using a large number of cells, we found that cAMP-treated ($n = 231$) and -untreated RCCs ($n = 82$) remained round-shaped and exhibited no obvious neurite outgrowth after several days of culture. Nevertheless, their mean capacitance (cell size) progressively increased with time independently of the exposure to pCPT-cAMP, suggesting that cAMP treatment had no major effects on morphology and cell size (Fig. 3*A*). In spite of this, the amplitude of T-type currents markedly increased with time and reached maximal values (93.1 ± 7.9 pA) 5 days after the cells' exposure to cAMP (6th day in culture). Normalization of current amplitudes by the cell capacitance gave current densities that increased by about 150% and reached a maximum after 4 days (Fig. 3*C*). Thus, for the remaining part of the experiments we used RCCs of more than 4 days after addition of cAMP and found that 78% of RCCs exposed to cAMP expressed T-type current densities of 6.2 ± 0.6 pA pF^{-1} (Fig. 3*C*) at −30 mV, which compared well with the L-type current densities available at +10 mV from $V_h = -40$ mV (7.2 ± 0.7 pA pF^{-1}, Fig. 3*D*) (see below). Notice also that in the 9% of cAMP-untreated cells exhibiting fast inactivating currents, the density of T-type channels at −30 mV was significantly smaller than in cAMP-treated RCCs (2.4 ± 0.1 pA pF^{-1}, $P < 0.001$).

In another series of experiments we examined whether HVA currents were affected by long-term incubations with cAMP. With holding potentials of −40 mV to avoid the contribution of T-type channels, the HVA current densities had comparable amplitudes in cAMP-treated and cAMP-untreated RCCs (Fig. 3*D*). Nifedipine

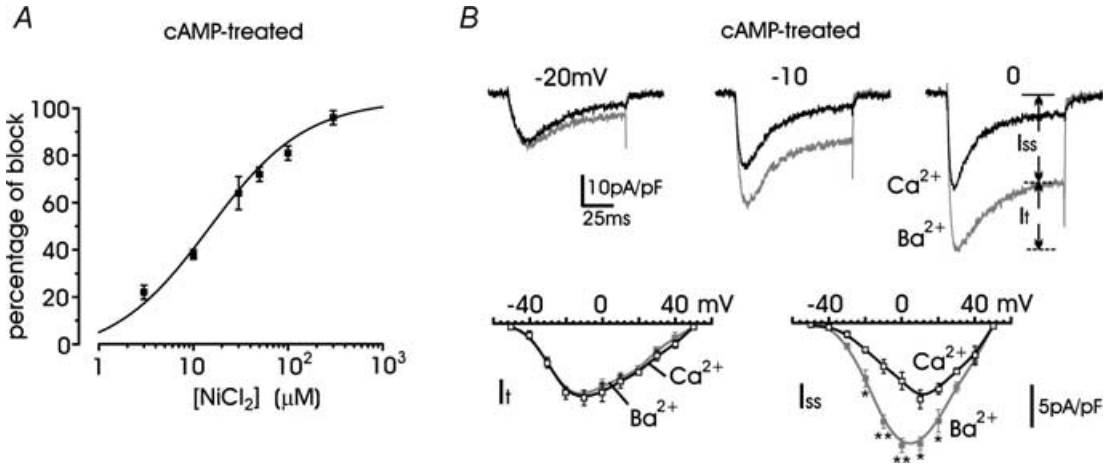

Figure 2. The transient current component of cAMP-treated RCCs is blocked by low doses of Ni^{2+} and is carried equally by Ca^{2+} and Ba^{2+}

A, dose–response relationship of Ni^{2+} block of the transient current component. Percentage of block was measured at either −30 or −20 mV and calculated from $n = 5$–10 values for each concentration. The smooth curve represents the fit to the data with $IC_{50} = 16.1 \pm 3.1$ μM and Hill slope 0.72 ± 0.11. *B*: upper traces, Ca^{2+} (black traces) and Ba^{2+} currents (grey traces) recorded at the potentials indicated from the same cAMP-treated RCC; lower traces, *I–V* relationships for the transient (I_t) and steady-state component (I_{ss}) of Ca^{2+} and Ba^{2+} currents evaluated at the end of a pulse, as indicated in the top panel. Step depolarizations of 10 mV increments starting from −50 mV were applied from a −80 mV holding potential. $^*P < 0.05$ and $^{**}P < 0.01$.

(1 μM) blocked an equal fraction of current densities in both cases (61 ± 7% and 62 ± 6%, respectively), suggesting that 4 days after cAMP exposure, L- and non-L-currents were unaltered. Notice also that the up-regulatory effects of cAMP on L-type channels (Carabelli *et al.* 2001; Cesetti *et al.* 2003) were not observed under these conditions because the cells were rinsed for several minutes before Ca^{2+} current recordings, and intracellular cAMP declines quickly following external cAMP (or isoprenaline) removal (Goaillard *et al.* 2001).

Biophysical properties of cAMP-recruited T-type channels

T-type channels are sensitive to preconditioning depolarizations, which induce a variable degree of voltage-dependent channel inactivation. The voltage dependence of T-type channel inactivation (channel availability) was evaluated using 500 ms depolarizations from −80 to −20 mV, preceding a test potential to −30 mV. As shown in Fig. 4*A* (■), T-type channel availability followed a single Boltzmann relation with $V_{1/2} = -45.9$ mV and steep voltage dependence ($k = 5.3$ mV).

T-type channels are also uniquely defined by the voltage dependence of their activation, inactivation and deactivation kinetics, which helps distinguish them from HVA channels, in particular from R-types (Randall & Tsien, 1997). With respect to these channels, the T-types possess slower activation and faster inactivation time courses. To isolate T-type currents from the total, the current traces of cAMP-treated cells were corrected for the Ni^{2+}-insensitive currents persisting after addition of 50 μM Ni^{2+}. Given the reported sensitivity of R-type currents to Ni^{2+} (Zamponi *et al.* 1996), for this analysis we selected RCCs which expressed large T-type currents that accounted for most of the fast inactivation, and the analysis was limited to the potential range −40 to +10 mV.

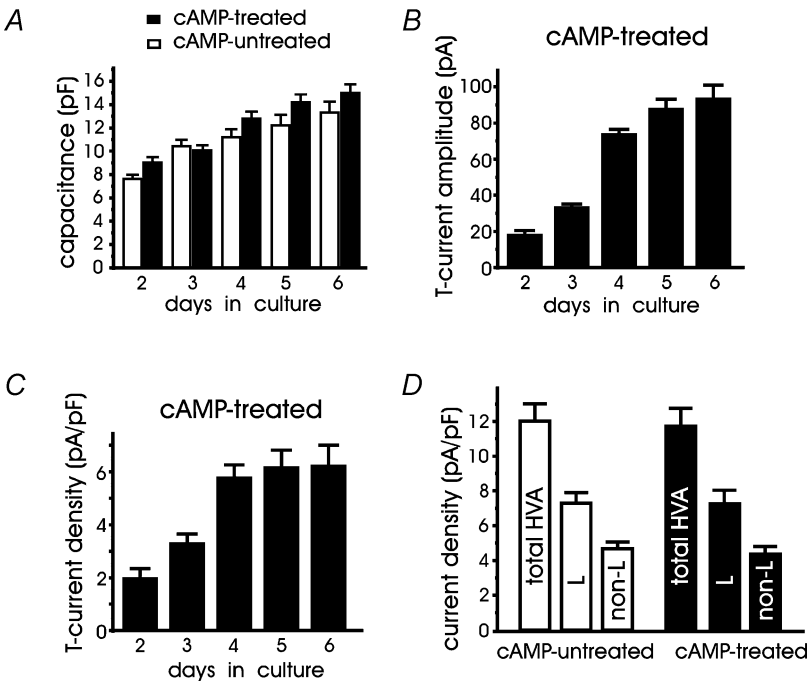

Figure 3. Cell capacitance and T-type current density increase with time in culture
A, in cAMP-untreated (open columns) and cAMP-treated RCCs (filled columns) the mean membrane capacitance increased equally with time in culture. The large number of RCCs used ($39 < n < 56$ and $12 < n < 24$ for cAMP-untreated and cAMP-treated cells, respectively) were selected randomly with no specific bias toward their size. *B*, mean T-type current amplitudes measured at −30 mV in RCCs exposed to pCPT-cAMP during the 1st day of culture. Notice the saturating size after the 5th day in culture (4th day after cAMP application). *C*, mean T-type current densities (in pA pF^{-1}) obtained by dividing the values of panel *B* by the values of panel *A*. *D*, mean current densities of total HVA, L- and non-L-type currents in cAMP-untreated (open columns, $n = 23$ cells) and cAMP-treated cells (filled columns, $n = 14$ cells). Current amplitudes were estimated from RCCs cultured for 5 days during step depolarizations to +10 mV from $V_h = -40$ mV to avoid contamination of T-type currents. The amplitude of L- and non-L-type currents was estimated by using 1 μM nifedipine (see text).

Figure 4*A–C* shows the conductance (g/g_{max}), the rise time of activation ($t_{10\text{-}90}$) and the time constant of inactivation (τ_{inact}) of Ni^{2+}-sensitive currents between −60 and +10 mV (●). Notice the low threshold and steep voltage dependence of channel conductance ($V_{1/2} = -27.4$ mV, $k = 7.7$ mV in 10 mM Ca^{2+}), the asymptotic values of τ_{inact} (18.3 ms) and rise time of activation (2.2 ms) at potentials above 0 mV, which are in good agreement with previously reported values of T-type channels in neurones and neuroendocrine cells (see Perez-Reyes, 2003).

The main singularity of T-type channels is their abnormally slow deactivation kinetics (Carbone & Lux, 1984*b*; Armstrong & Matteson, 1985). In cAMP-untreated cells, tail currents to either –110 or −50 mV from a −10 mV test potential were fast and well fitted by single exponentials (Fig. 5*A*). Time constants of deactivation (τ_{deact}) increased with increasing return potential (0.25 ms at −110 mV and 0.41 ms at −50 mV) and remained below 0.6 ms at −40 mV (▲ in Fig. 5*C*). In cAMP-treated cells, the tail at −50 mV was about 4-fold slower than that at −110 mV ($\tau_{deact} = 4.6$ ms and 1.1 ms, respectively; Fig. 5*B*). τ_{deact} was always greater than 0.9 ms and increased exponentially to reach mean values of 6.3 ms at −40 mV (● in Fig. 5*C*). There was also distinct voltage dependence of τ_{deact} in cAMP-untreated and cAMP-treated cells (e-fold change for 35.1 mV and 25.9 mV, respectively), suggesting the existence of distinct Ca^{2+} channel types in the two conditions.

Pharmacological isolation of cAMP-recruited T-type channels using Ca^{2+} channel blockers

We also attempted the isolation of T-type currents by blocking L-, N- and P/Q-type channels with solutions containing nifedipine (1 μM), ω-Aga-IVA (2 μM) and ω-CTx-GVIA (3.2 μM). RCCs were first preincubated for 10 min in Tyrode solution containing ω-Aga-IVA and ω-CTx-GVIA and then bathed in the presence of nifedipine. Most of the cAMP- and ω-toxin-treated RCCs displayed Ca^{2+} currents and *I–V* curves of the type illustrated in Fig. 6*A* (black traces), indicating the coexistence of T-type and ω-toxin-resistant R-type channels. The former contributed to the slowly activating and fast inactivating LVA current, visible at −30 and +20 mV in cAMP-treated cells (middle panel), and the latter contributed to the fast activating and slowly inactivating currents, more visible in cAMP-untreated cells (bottom panel). Notice how the R-type channels in cAMP-untreated cells activated quickly at −30 mV (more than 2-fold faster than T-type channels) despite the current being markedly small.

Better separation of T- from R-type channels could not be achieved even after applying SNX-482 (0.1–1 μM), a

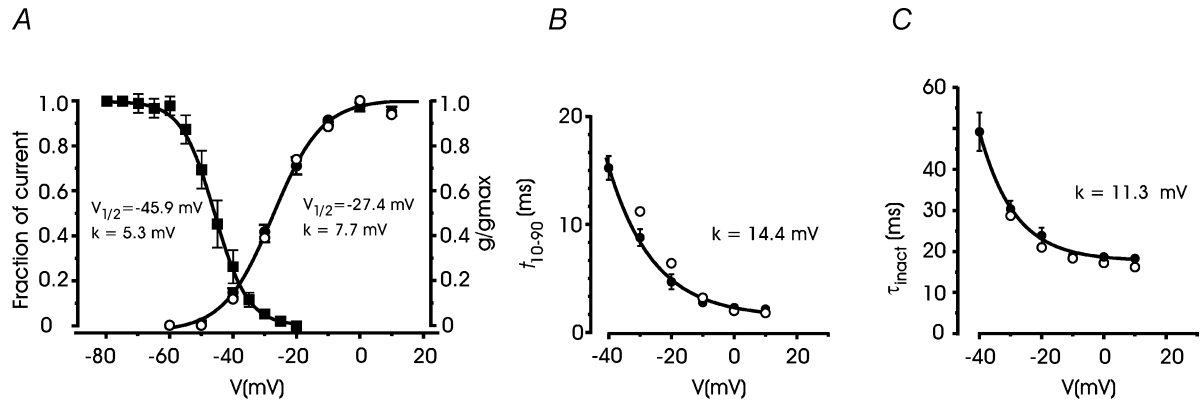

Figure 4. Activation and inactivation characteristics of cAMP-recruited T-type currents
A, steady-state inactivation and voltage dependent conductance of T-type currents. The inactivation curve (■) was obtained from $n = 8$ cAMP-treated cells using an inactivating prepulse of 500 ms (V_p) varying from −80 to −20 mV with 5 mV step increments. Test potential was to −30 mV. The continuous curve is a Boltzmann function best fitting the data points with $V_{1/2}$ and k as indicated. The normalized Ca^{2+} channel conductance (●) was calculated as $I_{peak}/(V - V_{rev})$ with $V_{rev} = +55$ mV from $n = 8$ cAMP-treated RCCs corrected for Ni^{2+}-insensitive currents. ○, data taken from the recordings of Fig. 6*B*. The continuous curve is a Boltzmann function with $V_{1/2}$ and k as indicated. *B* and *C*, voltage dependence of activation and inactivation. The former was measured as the time taken to rise from 10% to 90% of peak current ($t_{10–90}$), the latter by the inactivation time constant (τ_{inact}) calculated by fitting the decaying part of the currents with a single exponential, after Ni^{2+} correction, from $n = 8$ cAMP-treated cells (●). Smooth curves are single exponentials with k as indicated. Note the nice agreement between the mean values of the analysis (●) and the values derived from the recordings of Fig. 6*B* (○).

toxin reported to be selective for class E (R-type) channels (Newcomb *et al.* 1998). Acute applications of the toxin for 2–5 min at increasing concentrations (0.1, 0.3 and 1 μM) produced only small decrements (10–20%) of the current measured at the end of a 100 ms pulse to +10 mV, mainly associated with R-type channels ($n = 12$ cells; not shown). Block of R-type channels could not be achieved even after cell preincubation with SNX-482 in Tyrode solution (1 μM for 10 min, $n = 10$ cells), except in one case in which T-type channels could be recorded in full isolation (Fig. 6*B*), most likely because the cell lacked R-type channels. In fact, the cAMP-recruited current displayed the typical features of T-type currents over a wide range of potentials. The voltage dependence of conductance, rise time of activation, and inactivation time constant were comparable with those derived from the previous analysis (open *versus* filled circles in Fig. 4*A*–*C*).

Taken together, these findings support the idea that cAMP-recruited T-type channels generate a 'low-threshold shoulder' during ramp commands and well-identified 'slowly activating, fast inactivating' currents during step depolarizations to −30 and −20 mV. These were the main criteria we adopted to evaluate the presence of T-type channels in the following experiments.

β-AR stimulation and adenylate cyclase activation mimic the action of pCPT-cAMP

Cultured RCCs express β_1-ARs and β_2-ARs, which respond differently when stimulated with isoprenaline (ISO) (Cesetti *et al.* 2003). β_1-ARs act by selectively up-regulating L-type channel gatings through a cAMP/PKA-mediated pathway. β_2-ARs produce fast inhibition of L- and non-L-type channels through the activation of PTX-sensitive G proteins. Given the existence of an endogenous mechanism capable of raising cAMP in RCCs, we promptly tested whether the unselective stimulation of β-ARs with ISO (1 μM) or the selective stimulation of β_1-ARs with ISO plus 0.1 μM ICI 118.551 (a β_2-AR-selective antagonist) could induce the recruitment of T-type channels. We found that β-AR (or β_1-AR) stimulation was almost as effective as cAMP in recruiting T-type currents. Sixty-one per cent of RCCs exposed to ISO or ISO + ICI 118.551 displayed mixtures of LVA and HVA currents of the type illustrated in Fig. 7*A*. The LVA current had comparable amplitude (inset in Fig. 7*A*) and similar biophysical characteristics to the T-type currents recruited by cAMP. Higher responsiveness were obtained when RCCs were exposed to mixtures of the adenylate cyclase activator forskolin (10 μM) and the phosphodiesterase inhibitor IBMX (10 μM) (Fig. 7*B*), which produced enhanced levels of cAMP in most cells, as suggested by the marked increases of single L-type channel activity during short-term applications in cell-attached patches (T. Cesetti, P. Baldelli, J.-M. Hernández-Guijo & E. Carbone, unpublished observations). Forskolin + IBMX could recruit T-type current densities of standard amplitude in a fraction of RCCs comparable to cAMP (74% *versus* 78%, Fig. 7*A*). Thus, β-AR stimulation or adenylate cyclase activation were as effective as pCPT-cAMP in recruiting LVA currents in cultured RCCs.

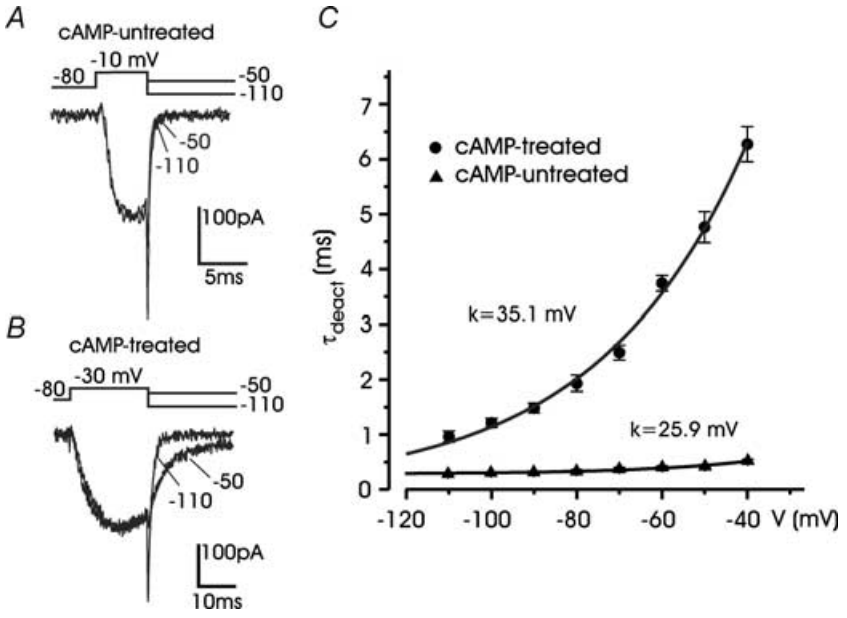

Figure 5. Deactivation of T-type and HVA currents
A, deactivation kinetics of HVA currents at −50 mV and −110 mV in a cAMP-untreated cell. Test depolarization was to −10 mV. The two tails were fitted with single exponentials (black traces) with time constants 0.41 ms (−50 mV) and 0.25 ms (− 110 mV). *B*, deactivation kinetics of a T-type current recorded from a cAMP-treated cell. Test depolarization was to −30 mV. Tail currents were fitted with single exponentials with time constant 4.6 ms (−50 mV) and 1.08 ms (−110 mV). *C*, voltage dependence of deactivation derived from $n = 8$ cAMP-treated cells (●) and $n = 8$ cAMP-untreated cells (▲). Note the progressive increase in the rate of tail current decay with more negative repolarization. Continuous lines are single exponential functions with e-fold changes (k) as indicated.

cAMP recruits newly available T-type channels mainly through a PKA-independent pathway

Given that ISO or forskolin + IBMX were able to mimic the action of pCPT-cAMP, the next issue was to examine whether the recruitment of T-type channels was mediated by a PKA-dependent or a PKA-independent pathway. To do this we tested the action of the PKA inhibitor H89 (0.3 μM) and the competitive antagonist of cAMP binding to PKA, Rp-cAMPS (0.5–1 mM). We found that both compounds had weak or no effects on the recruitment of T-type channels by pCPT-cAMP (Fig. 8*D*). H89 was apparently more effective in preventing T-type channel recruitment but the inhibitor also markedly reduced the amplitude of the HVA currents, suggesting an unspecific action on cell functioning. The action was even more unselective at higher concentrations ($> 1\ \mu$M) and became lethal at 10 μM ($n = 30$ cells). Given the partial selectivity of H89 towards PKA at concentrations $> 0.3\ \mu$M (see Davies *et al.* 2000) we attributed these effects to the unspecific inhibition of various protein kinases. On the contrary, we found the antagonistic action of Rp-cAMPS more reliable than H89. In 10 out of 13 RCCs (77%), we could detect T-type currents with mean amplitudes comparable to those induced by pCPT-cAMP (Fig. 8*A*).

We then examined whether the PKA-independent pathway mediated by the cAMP-receptor protein Epac (cAMP-GEF) was involved in the up-regulation of T-type channels. Epac binds cAMP at concentrations of $\sim$10 μM, mediates PKA-independent effects on various cell functions (Bos, 2003) and is selectively activated by the agonist 8CPT-2Me-cAMP (Enserink *et al.* 2002). In the majority of cells tested, 8CPT-2Me-cAMP (200 μM) reproduced the action of pCPT-cAMP (Fig. 8*B*). Fourteen out of 18 cells (78%) expressed T-type currents of comparable amplitudes to those induced by pCPT-cAMP, with the characteristic 'low-threshold shoulder' on the *I–V* curve and a prominent fast inactivating component at −20 and +20 mV (Fig. 8*B*).

Given that the action of pCPT-cAMP on T-type channel recruitment was mainly PKA-independent, we

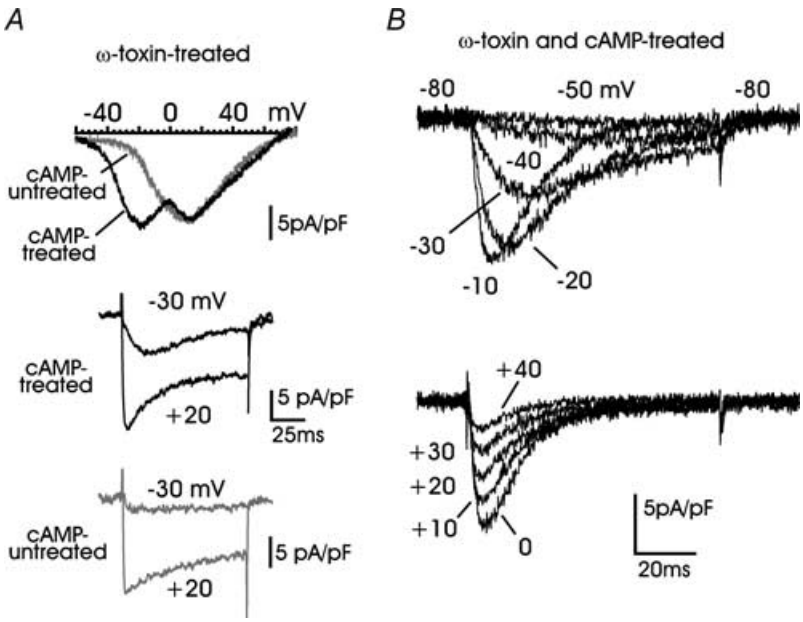

Figure 6. Pharmacological isolation of cAMP-recruited T-type currents
A: top panel, examples of *I–V* curves from cAMP-treated and cAMP-untreated cells preincubated with 3.2 μM ω-CTx-GVIA, 2 μM ω-Aga-IVA and bathed with 1 μM nifedipine. The two peaks at −22 mV and +12 mV in cAMP-treated cells (black trace) are associated with T-type and R-type channels, respectively. In cAMP-untreated cells only the *I–V* curve associated to HVA R-type channels is evident (grey trace); middle and bottom panels, two representative recordings of Ca^{2+} currents at −30 and +20 mV from ω-toxin-treated RCCs, which were cAMP-treated or cAMP-untreated. Note the presence of the cAMP-recruited T-type channels which activate slowly and inactivate almost fully at the end of the −30 mV pulse, in contrast to the fast activating and slowly inactivating current at the same potential in cAMP-untreated cells. *B*, time course of T-type currents recorded from a cell incubated with 3.2 μM ω-CTx-GVIA, 2 μM ω-Aga-IVA, 1 μM SNX-482 (10 min) and bathed with 1 μM nifedipine in which HVA channels appeared fully blocked. Notice the crossing over of the currents between −50 and −10 mV (upper panel) and the nearly constant rate of inactivation above 0 mV (lower panel).

next examined whether protein neosynthesis was involved in this mechanism. To do this, we tested the action of the protein synthesis inhibitor anisomycin (10 μM) by exposing the RCCs to the inhibitor for only 48 h to avoid its main toxic effects. Anisomycin was very effective in preventing the recruitment of T-type currents in most cells (18 out of 20). There was no clear evidence of fast inactivating currents at −20 mV and the *I–V* curve showed no sign of the 'low-threshold shoulder' (Fig. 8*C*). The remaining HVA currents appeared similar to those of cAMP-untreated cells, proving that anisomycin acted selectively on the recruitment of new T-type channels, without affecting the already available HVA currents. Finally, we examined whether the recruitment of T-type channels by cAMP could also possibly involve a calmodulin kinase II (CaMKII) pathway. To check this, the RCCs were incubated with KN-93, a selective inhibitor of CaMKII (Sumi *et al.* 1991), which was applied together with pCPT-cAMP and added again 24 h later. In 10 out of 10 RCCs, KN-93 (1 μM) was unable to prevent the recruitment of T-type channels. These displayed mean amplitudes comparable with those of the cAMP-treated cells shown in Fig. 1.

cAMP-recruited T-type channels change the threshold of burst firing in RCCs

In excitable cells, sufficient densities of T-type channels are able to lower the threshold of action potential generation and change the burst-firing pattern (Huguenard, 1996). To test whether this was the case in cAMP-treated RCCs, we examined the properties of action potential generation in cells maintained near physiological conditions (see Methods). RCCs were bathed in Tyrode solution containing 2 mM Ca^{2+}, 140 mM Na^{+} and recorded in the perforated patch configuration with the pipette containing 140 mM potassium aspartate to preserve high levels of intracellular K^{+}. Under these conditions the resting potential was set to −60 mV and a minimal injection current of 8 pA was required to generate action potentials in cAMP-untreated RCCs. Increasing currents produced an increased number of action potentials and shorter time delays to the first spike that reached asymptotic values with current injections > 20 pA (top traces in Fig. 9*A* and grey squares in Fig. 9*B*). In cAMP-treated RCCs, current injections of 5 pA were sufficient to produce single or multiple spikes (bottom traces in Fig. 9*A* and black triangles in Fig. 9*B*) and the delays were always shorter than cAMP-untreated RCCs, most likely due to the presence of newly recruited T-type channels, which were expected to contribute significantly around −40 mV in 2 mM Ca^{2+}.

To enhance the contribution of LVA channels to the firing properties of RCCs, a second series of experiments was performed at a holding potential of −90 mV by injecting small negative steady currents (Fig. 10). In cAMP-untreated cells, with step injections of 20 pA, the estimated threshold of action potential firing was -30.8 ± 0.19 mV ($n = 8$ cells), the overshoot amplitude 35.7 ± 0.9 mV, the half-width 3.6 ± 0.1 ms and the interpulse interval 73.1 ± 8.8 ms. In cAMP-treated RCCs, the recruitment of T-type channels markedly lowered the firing threshold to -39.0 ± 0.23 mV ($n = 8$; $P < 0.01$) and significantly increased the half-width (4.3 ± 0.1 ms; $P < 0.01$) (see Fig. 9*C*), while the overshoot amplitude (33.6 ± 0.7 mV;

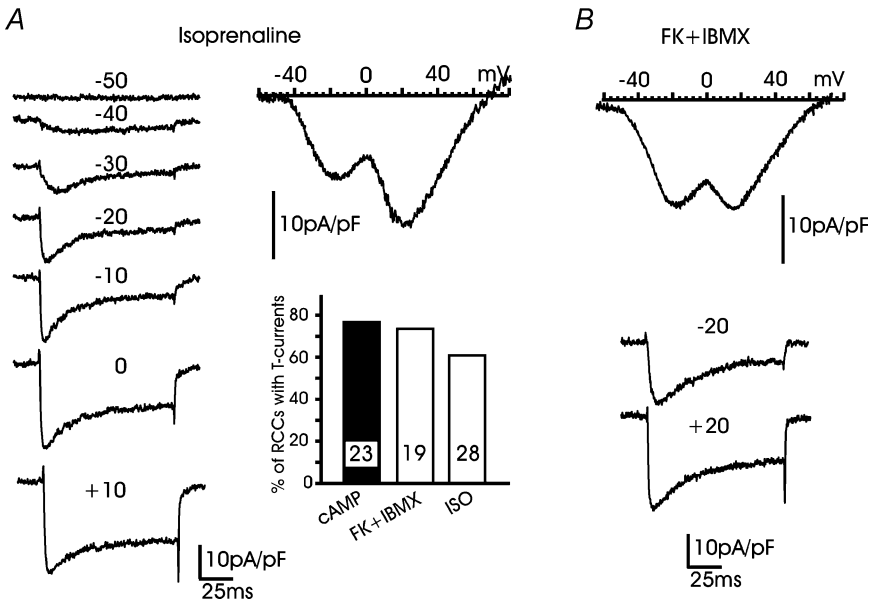

Figure 7. β-AR stimulation mimics the action of pCPT-cAMP
A, examples of *I–V* curve and current recordings from an RCC exposed to 1 μM isoprenaline (ISO) since the first day of culture. The ionic conditions were similar to those of Fig. 1*B*. Note the strong similarities with Ca^{2+} current recordings obtained from cAMP-treated cells. The bottom right graph reports the percentage of RCCs expressing T-type currents at −30 mV after exposure to pCPT-cAMP, forskolin + IBMX and ISO. Numbers within the columns indicate the number of RCCs examined. *B*, *I–V* curve and current traces at −20 mV and +20 mV from a cell expressing T-type currents following exposure to forskolin + IBMX.

$P < 0.2$) and the interpulse intervals remained relatively unchanged (67.8 ± 6.2 ms; $P < 0.6$). Notice that half of the cAMP-treated RCCs also expressed a small fraction of TTX-resistant Na^+ channels (20%). This current activated at more positive voltages with respect to T-type and Na-TTX-sensitive Na^+ channels ($V_{1/2}$ of activation -27.4 mV, -25.2 mV and -18.3 mV for T-type, TTX-sensitive and TTX-resistant Na^+ channels, respectively, in 10 mM Ca^{2+}) (M. Novara, P. Baldelli & E. Carbone unpublished results) and could thus contribute only marginally to the decreased firing threshold in cAMP-treated cells (see below).

Action potential firing associated with cAMP-recruited T-type channels

To identify the role of cAMP-recruited T-type channels we examined the action potential firing under different pharmacological conditions. In cAMP-untreated cells and in the presence of TTX (Fig. 10*A*), the spikes generated by the available HVA Ca^{2+} channels remained repetitive, had the same threshold of activation (-33.5 ± 2.5 mV) but exhibited lower peak amplitude (-1.8 ± 1.1 mV) and larger half-width (4.6 ± 0.15 ms; not shown). The addition of nifedipine (1 μM), ω-CTx-GVIA (3.2 μM) and ω-Aga-IVA (2 μM) to block L-, N- and P/Q-type channels almost completely abolished cell excitability, except during strong current injection (20 pA) at which the residual R-type channels were most likely activated. Replacement of Na^+ by $Tris^+$ resulted in the disappearance of action potentials, probably due to an approximately 10 mV junction potential shift caused by ion replacement.

The burst-firing pattern was significantly altered in eight cAMP-treated RCCs (Fig. 10*B*). In the presence of TTX, repetitive action potentials were available at a lower threshold (-38.7 ± 1.3 mV; $P < 0.05$), had larger half-widths (4.9 ± 0.1 mV; $P < 0.05$) but similarly low peak amplitudes (0.2 ± 2.4 mV) when compared to cAMP-untreated cells. Action potential bursts persisted also in the presence of $Tris^+$ and mixtures of Ca^{2+} channel blockers, indicating that cell excitability persisted even when Na^+ channels (TTX-sensitive and TTX-resistant) and most HVA Ca^{2+} channels were blocked in cAMP-treated cells. Under these conditions only T-type and R-type channels were available but, as shown by comparing

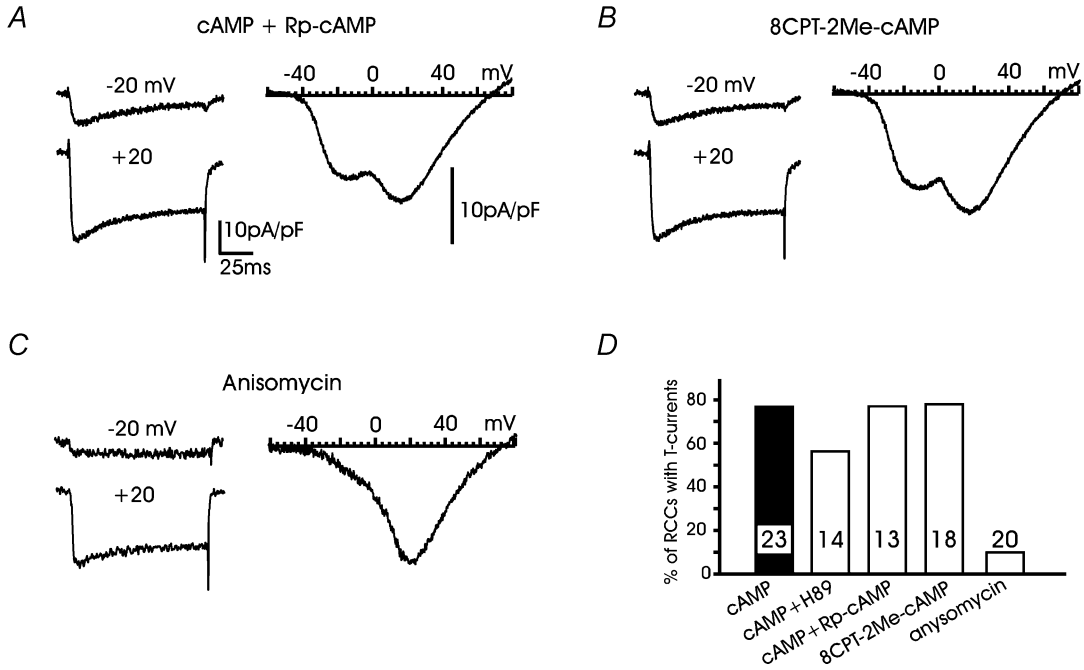

Figure 8. T-type channel recruitment is unaffected by Rp-cAMPS and 8CPT-2Me-cAMP but prevented by anisomycin

A and *B*, examples of *I–V* curves and Ca^{2+} currents in a cAMP-treated RCC incubated with either 200 μM pCPT-cAMP + 1 mM Rp-cAMPS or with 200 μM 8CPT-2Me-cAMP as indicated. Note the presence of transient T-type currents in both panels. *C*, examples of *I–V* curve and current traces showing no sign of T-type channels in a cAMP-treated cell incubated with the protein synthesis inhibitor anisomycin (10 μM for 48 h). Note the voltage dependence of nifedipine-insensitive channels remaining available. *D*, percentages of RCCs expressing T-type currents at -30 or -20 mV after exposures to: pCPT-cAMP + 0.3 μM H89, pCPT-cAMP + Rp-cAMPS, 8CPT-2Me-cAMP and anisomycin. The numbers of RCCs tested are indicated inside the columns.

Fig. 10*A* and *B*, the latter required higher current injection to generate all or none action potentials. Thus, the low-amplitude spikes shown in the bottom row of Fig. 10*B* were associated with the newly cAMP-recruited T-type channels. They were broader than Na^+ and HVA spikes (half-width 12.6 ± 0.57 ms *versus* 4.35 ± 0.10 ms; $P < 0.01$), peaked at lower potentials (-7.17 ± 1.14 mV) and disappeared in the presence of 200 μM Cd^{2+} (not shown).

Discussion

We have provided evidence that long-term exposures to pCPT-cAMP, β-AR stimulation or adenylate cyclase activators are capable of recruiting considerable densities of T-type channels, which are weakly expressed in cultured RCCs. The action of cAMP requires several days to reach maximal effects and leads to an effective increase of cell excitability. Given the presence of β-ARs in a large fraction of RCCs (Cesetti *et al.* 2003) and the tight arrangement of chromaffin cells in the adrenal gland, this implies that prolonged sympathetic stimulations can initiate a positive feedback loop capable of raising the cAMP levels, the neosynthesis of T-type channels and the remodelling of RCC excitability.

Biophysical properties of cAMP-recruited T-type channels

Evidence in favour of the expression of newly available T-type channels is unequivocal. First, the cAMP-recruited channels give rise to a transient Ca^{2+} current, peaking at around -20 mV. Inactivation is slow at -40 mV, accelerates at higher voltages reaching

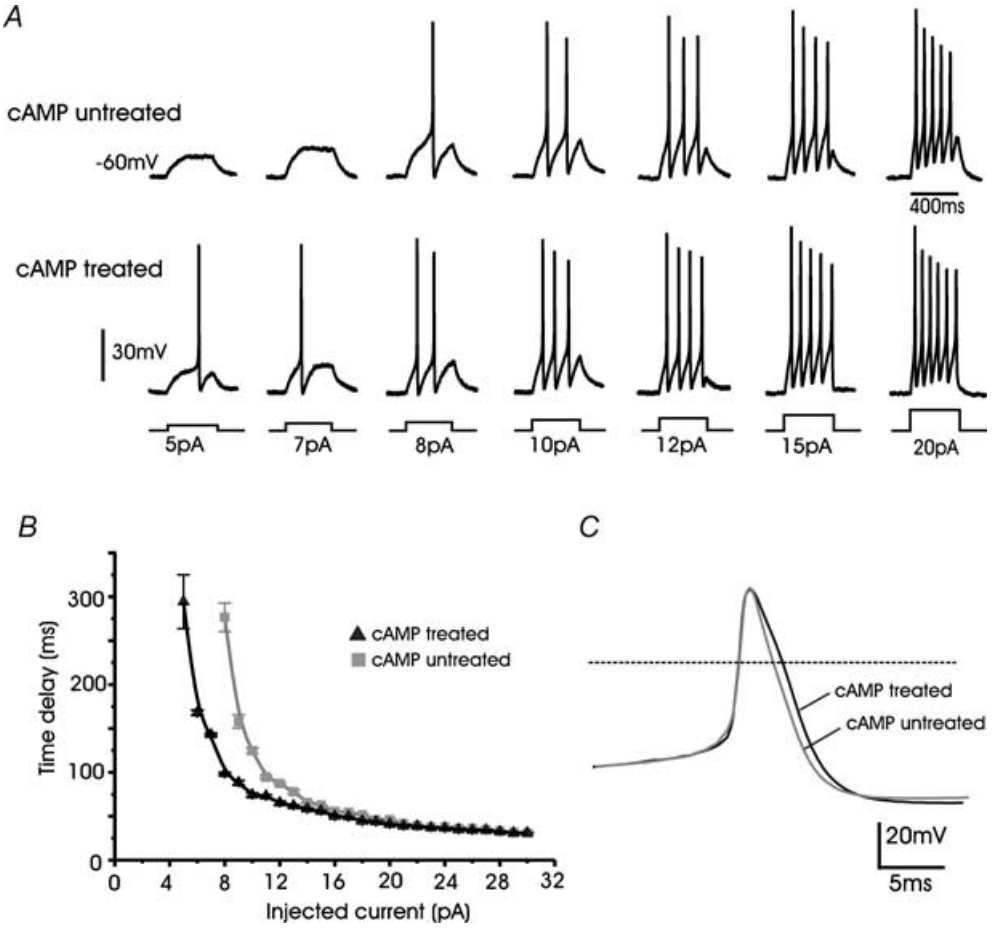

Figure 9. cAMP-recruited T-type channels modify the threshold of action potential firings in RCCs
A, action potential recordings from a cAMP-untreated (upper traces) and a cAMP-treated RCC (lower traces) during increasing current-clamp stimulations (5–20 pA). Cells were held at -60 mV by injecting 2–3 pA. Note that in the cAMP-treated cell, 5 pA was sufficient to elicit a spike, while in the cAMP-untreated cell 8 pA was required. *B*, mean time delay calculated from the start of the current pulse to the rise of the action potential for cAMP-treated ($n = 6$) and cAMP-untreated cells ($n = 7$). *C*, action potentials recorded on a time-expanded scale from cAMP-treated and cAMP-untreated RCCs showing the moderate broadening induced by cell exposure to pCPT-cAMP.

asymptotic values at +10 mV (18–20 ms). This is typical of native (Carbone & Lux, 1987) and cloned T-type channels (Cribbs *et al.* 1998; Perez-Reyes *et al.* 1998; Serrano *et al.* 1999; Kozlov *et al.* 1999). Second, T-type channels in RCCs possess the steady-state inactivation properties of LVA channels with $V_{1/2}$ at −46 mV and $k = 5.3$ mV, in full agreement with previously reported values (Perez-Reyes, 2003). Third, cAMP-recruited T-type channels are equally permeable to Ca^{2+} and Ba^{2+} (Carbone & Lux, 1987) and sensitive to low doses of Ni^{2+} (Fox *et al.* 1987). The IC_{50} of Ni^{2+} block in 10 mM Ca^{2+} (16 μM) is comparable to that of the α_{1H} ($Ca_V3.2$) channel isoform expressed in HEK-293 cells which is the Ca_V3 α_1-subunit most sensitive to Ni^{2+} (IC_{50} 13 μM in 10 mM Ba^{2+}; Lee *et al.* 1999), in agreement with the observation that cells of the adrenal glomerulosa possess α_{1H} channels (Schrier *et al.* 2001) and BCCs express the mRNA of $\alpha_{1G\text{-}H}$ (García-Palomero *et al.* 2000) . At- present, we do not have any direct evidence of a cAMP-mediated recruitment of α_{1H} (or α_{1G}) in RCCs. This would be interesting but not conditional to the main conclusion of the work. Fourth, cAMP-recruited T-type currents deactivate about 10 times more slowly than the HVA channels and are unlikely to be confused with the high-threshold R-type channels, which activate more rapidly between −40 and −20 mV, but inactivate more slowly and incompletely (Fig. 6). Fifth, T-type currents in RCCs were nearly unaffected by the addition of 30 μM Cd^{2+} (Fig. 1*D*), while R-type channels are largely blocked at these Cd^{2+} concentrations (Zhang *et al.* 1993; Tottene *et al.* 1996; Magnelli *et al.* 1998). Finally, cAMP-recruited LVA channels strongly resemble the T-type channels expressed in 50% of immature RCCs (Bournaud *et al.* 2001): (1) inactivation is steeply voltage dependent; (2) activation and steady-state inactivation have comparable $V_{1/2}$ values (−31.7 mV and −50.7 mV, in embryonic, *versus* −27.4 mV and −45.9 mV, in adult RCCs); and (3) channels deactivate slowly with comparable time constants. It is curious, however, that T-type channels expressed during development disappear in mature RCCs. Most likely, this could be due to a lowering of basal cAMP during cell maturation.

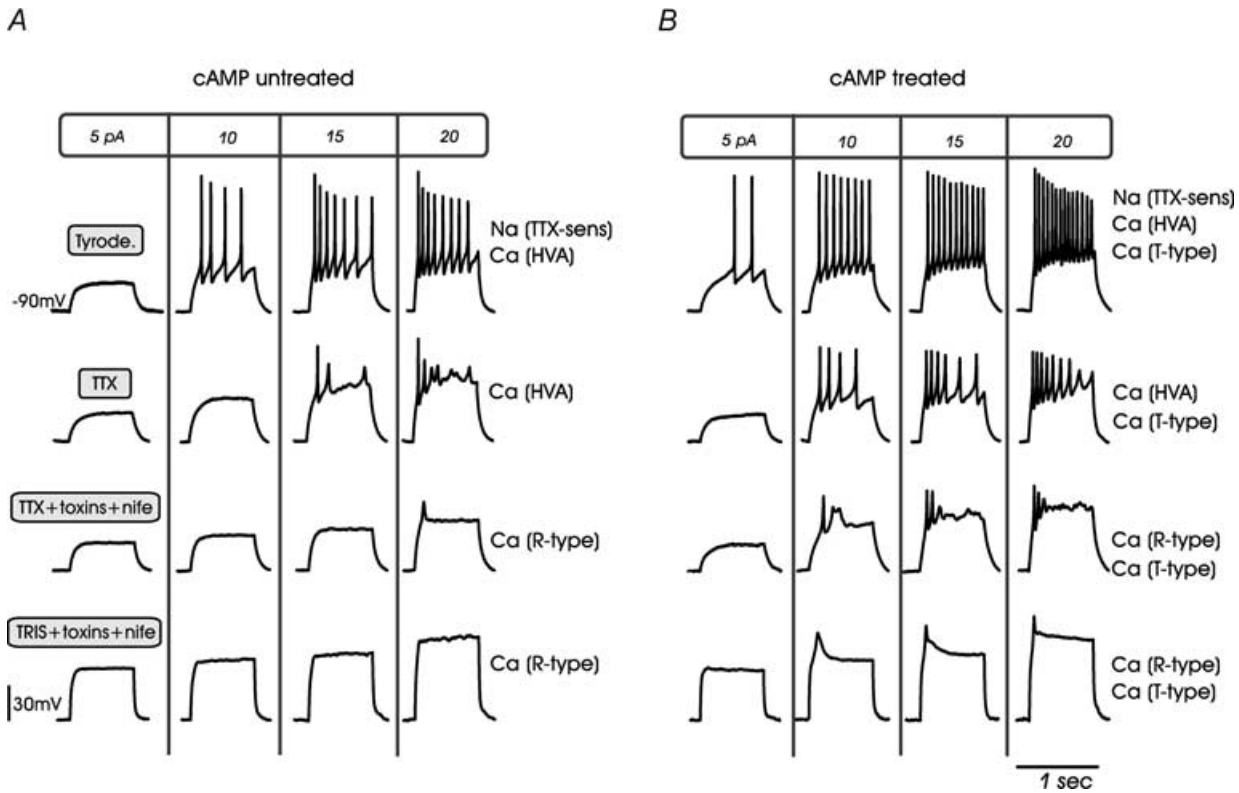

Figure 10. cAMP-recruited T-type channels modify the threshold of action potential firings in RCCs
Representative action potential recordings from cAMP-untreated *(A)* and cAMP-treated RCCs *(B)* under different Na^+ and Ca^{2+} channel-blocking conditions. Cells were held at −90 mV to favour the contribution of T-type channels and were depolarized by current steps of 800 ms to the values indicated at the top of each column. The four rows of recordings refer, in order, to action potentials in Tyrode solution, in the presence of TTX, with TTX + nifedipine + ω-toxins and with Tris + nifedipine + ω-toxins (see text).

cAMP and T-type channel recruitment

Our data show that the selective recruitment of T-type channels in RCCs involves new channel protein synthesis. T-type currents are not expressed in most cAMP-untreated cells and the addition of cAMP, isoprenaline or forskolin plus IBMX promotes the appearance of robust T-type currents after 3–4 days. This is the time lag usually required by neurotrophins to up-regulate presynaptic Ca^{2+} channels in central neurones (Baldelli *et al.* 2002). Like neurotrophins, the cAMP-mediated recruitment of T-type channels is fully prevented by the protein synthesis inhibitor anisomycin.

cAMP acts mainly by recruiting T-type channels without altering the density of L- and non-L-types. This is curious, since the cAMP/PKA pathway potentiates L-type channel activity after brief β-AR stimulations (Carbone *et al.* 2001; Cesetti *et al.* 2003) but is unable to up-regulate the L-channel density over days. Most likely, the main result of raising cAMP in RCCs is that of selectively turning on the synthesis of T-type channels, increasing cell excitability and triggering the remodelling of RCCs into neuronal-like cells to better synchronize their secretory activity. This represents a new form of 'chromaffin cell plasticity' that also explains the selective action of cAMP on recruiting a subset of TTX-resistant Na^+ channels contributing to ~20% of total Na^+ currents in 50% of RCCs, with different kinetics from TTX-sensitive Na^+ channels (Novara *et al.* 2002). Interestingly, cAMP elevations promote the survival of spinal cord motoneurones (Hanson *et al.* 1998), spinal axon regeneration (Qiu *et al.* 2002) and mechanical hyperalgesia (Sluka, 1997), while selective up-regulation of T-type channels has been reported during neuronal injury (Chung *et al.* 1993) and absence epilepsy (Tsakiridou *et al.* 1995). In addition to this, long-term treatment with cAMP promotes the overexpression of α_{1H} T-type channels in differentiating prostate cancer cells (Mariot *et al.* 2002) and sustained β-AR stimulation markedly up regulates T-type currents in cultured cardiomyocytes (Zhang *et al.* 2002). This latter being very likely the cause of the increased expression of T-type channels in cardiac hypertrophy (Nuss & Houser, 1993) and heart failure (Sen & Smith, 1994).

A PKA-independent pathway mediating T-channel up-regulation

Our data indicate that a PKA-independent pathway is mainly responsible for T-type channel recruitment in most RCCs. Two PKA antagonists (H89 and Rp-cAMPS) at the appropriate concentrations were unable to prevent the recruitment of T-type channels induced by pCPT-cAMP, and the selective activator of the cAMP receptor protein Epac (cAMP-GEF) could mimic the action of pCPT-cAMP and isoprenaline. The partial antagonistic action of H89 above 0.3 μM could be due to unspecific effects of the PKA inhibitor that at higher concentrations may inhibit various kinases (Davies *et al.* 2000). Our data are in good agreement with previous reports showing that a cAMP-dependent pathway is involved in the recruitment of T-type channels in Schwann and neuroendocrine cells (Beaudu-Lange *et al.* 1998; Mariot *et al.* 2002), although both reports do not mention the existence of PKA-dependent or PKA-independent pathways. A PKA-independent down-regulation of the $\alpha 6$ subunit of $GABA_A$ receptors in mature rat cerebellar granule cells has also been shown (Thompson *et al.* 2000). Alternatively, a PKA-dependent pathway is proposed for the cAMP analogue dbcAMP-induced Na^+ channel recruitment in bovine adrenal chromaffin cells, but in this study the effects of the cAMP analogue and forskolin were prevented by 30 μM H89, which is quite an excessive concentration to support the specific involvement of PKA (Yuhi *et al.* 1996).

Our findings represent the first evidence for the involvement of a cAMP-receptor protein Epac (cAMP-GEF) in the up-regulation of voltage-gated channels in excitable cells. Epac1 and Epac2 (cAMP-GEFI and cAMP-GEFII) are cytosolic proteins that bind cAMP with high affinity and mediate a number of PKA-independent cell functions (Bos, 2003). For example, cAMP-GEFII regulates the release of insulin in pancreatic β-cells (Ozaki *et al.* 2000) by controlling the rapid fusion of secretory granules (Eliasson *et al.* 2003) while Epac1 regulates the integrin-mediated cell adhesion induced by β_2-AR in ovarian tumour cells (Rangarajan *et al.* 2003). Epacs are localized at the cytosol, plasmalemma, nuclear membrane and microtubules (Qiao *et al.* 2002; Shibasaki *et al.* 2004) and there is convincing evidence that PKA-independent activation of extracellular-signal-regulated kinase (ERK) (Hamelink *et al.* 2002; Laroche-Joubert *et al.* 2002) may be mediated by one or more Epacs (Lin *et al.* 2003; Bos, 2003). As ERK activation is a preliminary step for gene transcription and protein neosynthesis, it is likely that the recruitment of T-type channels derives critically from an Epac signalling pathway activated by cAMP. However, our findings do not exclude the alternative hypothesis that the T-type Ca_V3 α_1-subunit is already present at the endoplasmic reticulum and that channel recruitment is favoured by the increased availability of an HVA auxiliary subunit (β, $\alpha 2\delta$ or γ) that facilitates channel incorporation into the plasma-membrane (Bichet *et al.* 2000). Concerning this

possibility, the auxiliary subunits of native T-type channels have not yet been identified and data on the interactions between HVA auxiliary subunits and Ca_V3 α_1-isoforms are not yet conclusive (Perez-Reyes, 2003). An answer to these issues requires further work using specific molecular and biochemical approaches that appear extremely complex in RCCs due to the low number of cells available in the present cell culture conditions (see Methods).

Finally, our data do not exclude the possibility that transient increases of basal Ca^{2+}, as might occur during the cAMP up-regulation of L-type channels (Cesetti *et al.* 2003), could also be responsible for the recruitment of T-type channels. However, in a series of experiments with RCCs exposed to Bay K 8644 (1 μM) and depolarized over 1–2 days with 10–60 mM KCl and 2–10 mM Ca^{2+}, to induce sustained Ca^{2+} influxes, we found no recruitment of any Ca^{2+} channel types (not shown).

A physiological role for T-type channels in chromaffin cells

The up-regulation of T-type channels following β-AR stimulation opens new perspectives on the role of LVA channels in catecholamine release from chromaffin cells. T-type channels are usually involved in lowering the threshold and changing the pattern of action potential firing in excitable cells (Huguenard, 1996). In RCCs, the presence of newly available LVA channels lowers the threshold of burst firing and increases cell excitability (Figs 9 and 10) with consequent elevation of Ca^{2+} entry and neurotransmitter release at low voltages. In this framework, the T-type channel recruitment associated with elevations of cAMP during β_1-AR stimulation represents a new constituent of the molecular apparatus controlling chromaffin cell activity. RCCs express sufficient densities of β_1-ARs (Cesetti *et al.* 2003), whose activation produces short-term cAMP elevations and marked exocytosis, with moderate increases of L-type currents (Carabelli *et al.* 2003). In this case, the long-term recruitment of T-type channels would further potentiate the positive feedback of catecholamine secretion, β-AR activation and cAMP production by enhancing Ca^{2+} entry at low voltages. Note that while T-type channels in immature RCCs are unable to induce secretion (Bournaud *et al.* 2001), the cAMP-recruited T-type channels of adult animals are effectively coupled to exocytosis (Giancippoli *et al.* 2004). This argues in favour of a novel functional role for LVA channels in catecholamine release, supported by the highly packed columnar arrangement of chromaffin cells in adrenal glands that could already be effective under normal physiological conditions.

References

Albillos A, Artalejo AR, López MG, Gandía L, García AG & Carbone E (1994). Ca^{2+} channel subtypes in cat chromaffin cells. *J Physiol* **477**, 197–213.

Albillos A, Neher E & Moser T (2000). R-type Ca^{2+} channels are coupled to the rapid component of secretion in mouse adrenal slice chromaffin cells. *J Neurosci* **20**, 8323–8330.

Almers W & McCleskey EW (1984). Non-selective conductance in calcium channels of frog muscle: calcium selectivity in a single file pore. *J Physiol* **353**, 585–608.

Armstrong CM & Matteson DR (1985). Two distinct populations of calcium channels in a clonal line of pituitary cells. *Science* **227**, 65–67.

Artalejo CR, Adams ME & Fox AP (1994). Three types of Ca^{2+} channel trigger secretion with different efficacies in chromaffin cells. *Nature* **367**, 72–76.

Baldelli P, Novara M, Carabelli V, Hernández-Guijo JM & Carbone E (2002). BDNF up-regulates evoked GABAergic transmission in developing hippocampus by potentiating presynaptic N- and P/Q-type Ca^{2+} channels signalling. *Eur J Neurosci* **16**, 2397–2310.

Barbara JG & Takeda K (1995). Voltage-dependent currents and modulation of calcium channel expression in zona fasciculata cells from rat adrenal gland. *J Physiol* **488**, 609–622.

Beaudu-Lange C, Despeyroux S, Marcaggi P, Coles JA & Amédée T (1998). Functional Ca^{2+} and Na^{+} channels on mouse Schwann cells cultured in serum-free medium: regulation by a diffusible factor from neurons and by cAMP. *Eur J Neurosci* **10**, 1796–1809.

Bichet D, Cornet V, Geib S, Carlier E, Volsen S, Hoshi T, Mori Y & De Waard M (2000). The I–II loop of the Ca^{2+} channel alpha1 subunit contains an endoplasmic reticulum retention signal antagonized by the beta subunit. *Neuron* **25**, 177–190.

Bos JL (2003). Epac: a new cAMP target and new avenues in cAMP research. *Nature Rev Mol Cell Biol* **4**, 733–738.

Bournaud R, Hidalgo J, Yu H, Jaimovich E & Shimahara T (2001). Low threshold T-type calcium current in rat embryonic chromaffin cells. *J Physiol* **537**, 35–44.

Carabelli V, Giancippoli A, Baldelli P, Carbone E & Artalejo AR (2003). Distinct potentiation of L-type currents and secretion by cAMP in rat chromaffin cells. *Biophys J* **85**, 1325–1337.

Carabelli V, Hernández-Guijo JM, Baldelli P & Carbone E (2001). Direct autocrine inhibition and cAMP-dependent potentiation of single L-type Ca^{2+} channels in bovine chromaffin cells. *J Physiol* **532**, 73–90.

Carbone E, Carabelli V, Cesetti T, Baldelli P, Hernández-Guijo JM & Giusta L (2001). G-protein- and cAMP-dependent L-channel gating modulation: a manyfold system to control calcium entry in neurosecretory cells. *Pflugers Arch* **442**, 801–813.

Carbone E & Lux HD (1984*a*). A low voltage-activated, fully inactivating Ca channel in vertebrate sensory neurons. *Nature* **310**, 501–502.

Carbone E & Lux HD (1984*b*). A low voltage-activated calcium conductance in embryonic chick sensory neurons. *Biophys J* **46**, 413–418.

Carbone E & Lux HD (1987). Kinetics and selectivity of a low-voltage-activated calcium current in chick and rat sensory neurones. *J Physiol* **386**, 547–570.

Cesetti T, Hernández-Guijo JM, Baldelli P, Carabelli V & Carbone E (2003). Opposite action of β_1- and β_2-adrenergic receptors on Ca_V1, L-channel current in rat adrenal chromaffin cells. *J Neurosci* **23**, 73–83.

Chung J-M, Huguenard JR & Prince DA (1993). Transient enhancement of low-threshold calcium current in thalamic relay after corticectomy. *J Neurophysiol* **702**, 20–27.

Cribbs LL, Lee J-H, Yang J, Satin J, Zhang Y, Daud A, Barclay J, Williamson MP, Fox M, Rees M & Perez-Reyes E (1998). Cloning and characterization of α_{1H} from human heart, a member of the T-type Ca^{2+} channel gene family. *Circ Res* **83**, 103–109.

Davies SP, Reddy H, Caivano M & Cohen P (2000). Specificity and mechanism of action of some commonly used protein kinase inhibitors. *Biochem J* **351**, 95–105.

Doležal V, Lisá V, Diebler M-F, Kašparová J & Tuček S (2001). Differentiation of NG108-15 cells induced by the combined presence of dbcAMP and dexamethasone brings about the expression of N and P/Q types of calcium channels and the inhibitory influence of muscarinic receptors on calcium influx. *Brain Res* **910**, 134–141.

Eliasson L, Ma X, Renström E, Barg S, Berggren P-O, Galvanovskis J, Gromada J, Jing X, Lundquist I, Salehi A, Sewing S & Rorsman P (2003). SUR1 regulates PKA-independent cAMP-induced granule priming in mouse pancreatic B-cells. *J General Physiol* **121**, 183–197.

Engisch KL & Nowycky MC (1996). Calcium dependence of large dense-cored vesicle exocytosis evoked by calcium influx in bovine adrenal chromaffin cells. *J Neurosci* **16**, 1359–1369.

Enserink JM, Chrinstensen AE, de Rooij J, van Triest M, Schwede F, Gottfried Genieser H, Deskeland SO, Blank JL & Bos JL (2002). A novel Epac-specific cAMP analogue demonstrates independent regulation of Rap1 and ERK. *Nature Cell Biol* **4**, 901–906.

Fox AP, Nowycky MC & Tsien RW (1987). Kinetic and pharmacological properties distinguishing three types of calcium currents in chick sensory neurons. *J Physiol* **394**, 149–172.

Gandía L, Borges R, Albillos A & García AG (1995). Multiple calcium channel subtypes in isolated rat chromaffin cells. *Pflugers Arch* **430**, 55–63.

García AG, Sala F, Reig JA, Viniegra S, Frías J, Fonteriz RI & Gandía L (1984). Dihydropyridine Bay-K-8644 activates chromaffin cell calcium channels. *Nature* **309**, 69–71.

García-Palomero E, Cuchillo I, García AG, Renart J, Albillos A & Montiel C (2000). Greater diversity than previously thought of chromaffin cell Ca^{2+} channels, derived from mRNA identification studies. *FEBS Lett* **481**, 235–239.

Giancippoli A, Carabelli V, Novara M, Baldelli P, Cavallari D & Carbone E (2004). Exocytosis associated to T-type channels recruited by prolonged cAMP exposure in rat chromaffin cells. *Biophys J* **86**, 233A.

Goaillard J-M, Vincent P & Fischmeister R (2001). Simultaneous meaurements of intracellular cAMP and L-type Ca^{2+} current in single ventricular myocytes. *J Physiol* **530**, 79–91.

Hamelink C, Lee H-W, Chen Y, Grimaldi M & Eiden LE (2002). Coincident elevation of cAMP and calcium influx by PACAP-27 synergistically regulates vasoactive intestinal polypeptide gene transcription through a novel PKA-independent signaling pathway. *J Neurosci* **22**, 5310–5320.

Hanson MG, Shen S, Wiemelt AP, McMorris FA & Barres BA (1998). Cyclic AMP elevation is sufficient to promote the survival of spinal motor neurons *in vitro*. *J Neurosci* **18**, 7361–7371.

Hernández-Guijo JM, Carabelli V, Gandía L, García AG & Carbone E (1999). Voltage-independent autocrine modulation of L-type channels mediated by ATP, opioids and catecholamines in rat chromaffin cells. *Eur J Neurosci* **11**, 3574–3584.

Hollins B & Ikeda SR (1996). Inward currents underlying action potentials in rat adrenal chromaffin cells. *J Neurophysiol* **76**, 1195–1211.

Huguenard JR (1996). Low-threshold calcium currents in central neurons. *Annu Rev Physiol* **58**, 329–348.

Kozlov AS, McKenna F, Lee J-H, Cribbs LL, Perez-Reyes E, Feltz A & Lambert RC (1999). Distinct kinetics of cloned T-type Ca^{2+} channels lead to differential Ca^{2+} entry and frequency-dependence during mock action potentials. *Eur J Neurosci* **11**, 4149–4158.

Laroche-Joubert N, Marsy S, Michelet S, Imbert-Teboul M & Doucet A (2002). Protein kinase A-independent activation of ERK and H,K-ATPase by cAMP in native kidney cells. *J Biol Chem* **277**, 18598–18604.

Lee JH, Gomora JC, Cribbs LL & Perez-Reyes E (1999). Nickel block of three cloned T-type calcium channels: low concentrations selectively block α_{1H}. *Biophys J* **77**, 3034–3042.

Lin SL, Johnson-Farley NN, Lubinsky DR & Cowen DS (2003). Coupling of neuronal 5-HT_7 receptors to activation of extracellular-regulated kinase through a protein kinase A-independent pathway that can utilize Epac. *J Neurochem* **87**, 1076–1085.

Magnelli V, Baldelli P & Carbone E (1998). Antagonists-resistant calcium currents in rat embryo motoneurons. *Eur J Neurosci* **10**, 1810–1825.

Mariot P, Vanoverbergher K, Lalevée N, Rossier MF & Prevarskaya N (2002). Overexpression of an α_{1H} ($Ca_V3.2$) T-type calcium channel during neuroendocrine differentiation of human prostate cancer cells. *J Biol Chem* **277**, 10824–10833.

Newcomb R, Skoze B, Palma A, Wang G, Chen X, Hopkins W, Cong R, Miller J, Urge L, Tarczy-Hornoch K, Loo JA, Dooley DJ, Nadasdi L, Tsien RW, Lemos J & Miljanich G (1998). Selective peptide antagonist of the class E calcium channel from the venom of the tarantula *Histeroscates gigas*. *Biochemistry* **37**, 15353–15362.

Novara M, Baldelli P, Hernandez-Guijo JM, Giusta L & Carbone E (2002). Chronic exposure to cAMP upregulates T-type Ca^{2+} channels and TTX-insensitive Na^+ channels in cultured rat chromaffin cells. *J Physiol* **543.P**, 67*P*.

Nuss HB & Houser SR (1993). T-type Ca^{2+} current is expressed in hypertrophied adult feline left ventricular myocytes. *Circ Res* **73**, 777–782.

Ozaki N, Shibasaki T, Kashima Y, Miki T, Takahashi K, Ueno H, Sunaga Y, Yano H, Matsuura Y, Iwanaga T, Takai Y & Seino S (2000). cAMP-GEFII is a direct target of cAMP in regulated exocytosis. *Nature Cell Biol* **2**, 805–811.

Parramón M, González MP & Oset-Gasque MJ (1995). A reassessment of the modulatory role of cyclic AMP in catecholamine secretion by chromaffin cells. *Br J Pharmacol* **114**, 517–523.

Perez-Reyes E (2003). Molecular physiology of low-voltage-activated T-type calcium channels. *Physiol Rev* **83**, 117–161.

Perez-Reyes E, Cribbs LL, Daud A, Lacerda AE, Barclay J, Williamson MP, Fox M, Rees M & Lee JH (1998). Molecular characterization of a neuronal low-voltage-activated T-type calcium channel. *Nature* **391**, 806–900.

Qiao J, Mei FC, Popov V, Vergara L & Cheng X (2002). Cell cycle-dependent subcellular localization of exchanger factor directly activated by cAMP. *J Biol Chem* **277**, 26581–26586.

Qiu J, Cai D, Dai H, McAtee M, Hoffman PN, Bregman BS & Filbin MT (2002). Spinal axon regeneration induced by elevation of cyclic AMP. *Neuron* **34**, 895–903.

Randall AD & Tsien RW (1997). Contrasting biophysical and pharmacological properties of T-type and R-type calcium channels. *Neuropharmacol* **36**, 879–893.

Rangarajan S, Enserink JM, Kuiperij B, de Rooij J, Price LS, Schwede F & Bos JL (2003). Cyclic AMP induces integrin-mediated cell adhesion through Epac and Rap1 upon stimulation of the β_2-adrenergic receptor. *J Cell Biol* **160**, 487–493.

Schrier AD, Wang H, Talley EM, Perez-Reyes E & Barrett PQ (2001). α_{1H} T-type Ca^{2+} channel is the predominant subtype expressed in bovine and rat zona glomerulosa. *Am J Physiol Cell Physiol* **280**, C265–C272.

Sen L & Smith TW (1994). T-type Ca^{2+} channels are abnormal in genetically determined cardiomyopathic hamster hearts. *Circ Res* **75**, 149–155.

Serrano JR, Perez-Reyes E & Jones SW (1999). State-dependent inactivation of the α_{1G} T-type calcium channel. *J General Physiol* **114**, 185–201.

Shibasaki T, Sunaga Y, Fujimoto K, Kashima Y & Seino S (2004). Interaction of ATP sensor, cAMP sensor and voltage-dependent Ca^{2+} channel in insulin granule exocytosis. *J Biol Chem* **279**, 7956–7961.

Sluka KA (1997). Activation of the cAMP transduction cascade contributes to the mechanical hyperalgesia and allodynia induced by intradermal injection of capsaicin. *Br J Pharmacol* **122**, 1165–1173.

Sumi M, Kiuchi K, Ishikawa T, Ishii A, Hagiwara M, Nagatsu T & Hidaka H (1991). The newly synthesized selective Ca^{2+}/calmodulin dependent protein kinase II inhibitor KN-93 reduces dopamine contents in PC12h cells. *Biochem Biophys Res Commun* **181**, 968–975.

Thompson CL, Razzini G, Pollard S & Stephenson FA (2000). Cyclic AMP-mediated regulation of $GABA_A$ receptor subunit expression in mature rat cerebellar granule cells: evidence for transcriptional and translational control. *J Neurochem* **74**, 920–931.

Tottene A, Moretti A & Pietrobon D (1996). Functional diversity of P-type and R-type calcium channels in rat cerebellar neurons. *J Neurosci* **16**, 6353–6363.

Tsakiridou E, Bertollini L, de Curtis M, Avanzini G & Pape H-C (1995). Selective increase in T-type calcium conductance of reticular thalamic neurons in a rat model of absence epilepsy. *J Neurosci* **152**, 3110–3117.

Yuhi T, Wada A, Yamamoto R, Yanagita T & Hiromi N (1996). Up-regulation of functional voltage-dependent sodium channels by cyclic AMP-dependent protein kinase in adrenal medulla. *Brain Res* **709**, 37–43.

Zamponi GW, Bourinet E & Snutch TP (1996). Nickel block of a family of neuronal calcium channels: subtype- and subunit-dependent action at multiple sites. *J Membr Biol* **151**, 77–90.

Zhang J-F, Randall AD, Ellinor PT, Horne WA, Sather WA, Tanabe T, Schwarz TL & Tsien RW (1993). Distinctive pharmacology and kinetics of cloned neuronal Ca^{2+} channels and their possible counterparts in mammalian CNS neurons. *Neuropharmacol* **32**, 1075–1088.

Zhang L-M, Wang Z & Nattel S (2002). Effects of sustained β-adrenergic stimulation on ionic currents of cultured adult guinea pig cardiomyocytes. *Am J Physiol Heart Circ Physiol* **282**, H880–H889.

Acknowledgements

We wish to thank Dr J. M. Hernández-Guijo for helpful discussions. This work was supported by the Italian CNR (grant no. 01.00443.ST97) and MIUR (grant no. 2001055324-006).

Author's present address

P. Baldelli: Department of Experimental Medicine, Viale Benedetto XV, 3, 16132 Genova, Italy.